In-situ doped junctionless polysilicon nanowires field effect transistors for low-cost biosensors

Zulfiqar, Azeem; Patou, François; Pfreundt, Andrea; Papakonstantinopoulos, Charalampos; Svendsen, Winnie Edith; Dimaki, Maria

Published in:
Sensing and Bio-Sensing Research

Link to article, DOI:
10.1016/j.sbsr.2016.09.001

Publication date:
2017

Document Version
Publisher's PDF, also known as Version of record

Sensing and Bio-Sensing Research 13 (2017) 88–95

Contents lists available at ScienceDirect

Sensing and Bio-Sensing Research

journal homepage: www.elsevier.com/locate/sbsr

In-situ doped junctionless polysilicon nanowires field effect transistors for low-cost biosensors

Azeem Zulfiqar, François Patou, Andrea Pfreundt, Charalampos Papakonstantinopoulos, Winnie E. Svendsen, Maria Dimaki *

Technical University of Denmark, Nanotechnology Department, Ørsteds PladsBuilding 345B, 2800 Kgs. Lyngby, Denmark

ARTICLE INFO

Article history:
Received 1 July 2016
Received in revised form 30 August 2016
Accepted 6 September 2016

Keywords:
In-situ doped
Polysilicon nanowire
Field effect transistor
Biosensor

ABSTRACT

Silicon nanowire (SiNW) field effect transistor based biosensors have already been proven to be a promising tool to detect biomolecules. However, the most commonly used fabrication techniques involve expensive Silicon-On-Insulator (SOI) wafers, E-beam lithography and ion-implantation steps. In the work presented here, a top down approach to fabricate SiNW junctionless field effect biosensors using novel in-situ doped polysilicon is demonstrated. The p-type polysilicon is grown with an optimum boron concentration that gives a good metal-silicon electrical contact while maintaining the doping level at a low enough level to provide a good sensitivity for the biosensor. The silicon nanowires are patterned using standard photolithography and a wet etch method. The metal contacts are made from magnetron sputtered TiW and e-beam evaporation of gold. The passivation of electrodes has been done by sputtered Si_3N_4 which is patterned by a lift-off process. The characterization of the critical fabrication steps is done by Secondary Ion Mass Spectroscopy (SIMS) and by statistical analysis of the measurements made on the width of the SiNWs. The electrical characterization of the SiNW in air is done by sweeping the back gate voltage while keeping the source drain potential to a constant value and surface characterization is done by applying liquid gate in phosphate buffered saline (PBS) solution. The fabricated SiNWs sensors functionalized with (3-aminopropyl)triethoxysilane (APTES) have demonstrated good sensitivity in detecting different pH buffer solutions.

1. Introduction

Since the first demonstration of silicon nanowires (SiNWs) as biological field effect transistors in 2001 [1], where the detection of small concentrations of biomolecules down to 10 pM was demonstrated, a lot of advancements have been made in utilizing them as label-free sensors to detect viruses, cancers, DNA etc. [2–5]. This has opened up the possibility to implement SiNW biosensors in Point-Of-Care (POC) devices, that can play a major role in patient level diagnostics, personalized treatment, drug development, food safety and forensics [6–12] due to their compact size and small amount of required sample. In order to achieve this, a simple, low cost, highly reproducible and robust fabrication technique is needed that is also compatible with the existing commercial setups used for mass manufacturing of devices.

The bottom up fabrication technique that was originally used to produce SiNWs biosensors [13] has various limitations that include poor reproducibility, several inspection steps and slow production speed. These limitations were greatly improved by the implementation of top down fabrication techniques that use Silicon-On-Insulator (SOI) wafers [14–23] to fabricate SiNWs biosensors. However, these techniques involved expensive wafers i.e. SOI wafers with a thin device layer of single crystal silicon and expensive fabrication techniques like electron-beam and deep ultraviolet lithography. Some research groups have replaced the single crystal silicon device layer with polysilicon and have used photolithography instead of e-beam [24–27] to reduce the cost of substrate and the use of expensive equipment. However, no efforts have been made to further simplify the fabrication steps, e.g. the doping techniques of the silicon nanowire, which can also be rather time consuming and expensive. Steps like these are necessary in order to develop disposable POC devices.

Indeed, most fabrication techniques use differential doping in the SiNWs, where the source and drain are highly doped to get an ohmic contact between silicon (Si) and metal. This requires the use of the ion-implantation method, in which the dopants are implanted in the required regions and then driven in the silicon by high temperature annealing. The method is expensive, as not everyone has access to the required tool, and is also rather difficult to optimize.

In this paper in-situ boron doped polysilicon has been used for the fabrication of SiNWs biosensors in a junctionless transistor configuration [28]. The material is rather novel, as very few examples of sensing have been reported using it, and only on gas sensors [29]. As the

* Corresponding author.
E-mail address: maria.dimaki@nanotech.dtu.dk (M. Dimaki).

http://dx.doi.org/10.1016/j.sbsr.2016.09.001

depletion length of the silicon nanowire is inversely proportional to its doping concentration, a relatively low doping is needed to make sure that a 15–20 nm wire can be fully depleted. At the same time though, a very low doping concentration will give rise to barriers at the contact between metal and silicon, which is not wanted. Therefore, when using in-situ doped polysilicon, the doping concentration has to consider both limitations. A study on this has been done in this paper. In addition, the photolithography and wet etch patterning of SiNWs used in this paper make it possible to produce wafers with nanometer sized SiNWs in both height and width in a batch process. A detailed characterization of the fabrication process, which includes dopant concentration, wet etching and contact annealing, is done to ensure high yield and reproducibility of the SiNWs biosensors. The electrical characterization and liquid gate measurements show the transistor characteristics of these devices. Finally, the SiNWs have successfully been functionalized with (3-aminopropyl)triethoxysilane (APTES) and have demonstrated good sensitivity for pH sensing.

2. Materials and methods

The substrate wafer used for fabrication of silicon nanowires was 4 in., p-type, double sided polished wafer with crystal orientation ⟨100⟩, sheet resistance of 1–20 Ω-cm and thickness of around 350 μm supplied by OKMETIC (Finland). To functionalize the SiNWs (3-aminopropyl)triethoxysilane (APTES) and *N,N* Diisopropylethylamine (DIPA) were purchased from SIGMA ALDRICH. The pH buffer solutions for sensing experiments were prepared in the lab and the pH values were measured using a pH meter.

2.1. Fabrication of sensor

Step 1: The buried dielectric was formed on the substrate by growing a 30 nm thick layer of silicon dioxide (SiO_2) at 1100 °C followed by the deposition of 50 nm thick layer of stoichiometric silicon nitride (Si_3N_4) at around 800 °C by using two separate Tempress horizontal furnaces.

Step 2: The SiNW material was deposited on top of the Si_3N_4 by growing a 30 nm thick layer of in-situ doped p-type polysilicon with boron concentration of around 3–5 × 10^{18} atoms/cm^3 by using another Tempress horizontal furnace. The thickness of the polysilicon was then reduced to around 20 nm by 1 min dry oxidation followed by 20 min annealing at 1100 °C. The resulting thin SiO_2 layer was then removed by wet etching in Buffered Hydrofluoric Acid (BHF).

Step 3: The SiNWs were patterned through a wet etch process. 220 nm of silicon rich Plasma Enhanced Chemical Vapor Deposition (PECVD) Si_3N_4 were first deposited on the wafer and patterned by photolithography followed by a 1 min dry etch in the Induced Coupled Plasma (ICP) etch machine supplied by STS and a 5 min wet etch in BHF. This patterned Si_3N_4 with dimensions of length × width = 70 μm × 2 μm, length × width = 120 μm × 2 μm, length × width = 70 μm × 5 μm and length × width = 120 μm × 5 μm was used as an etch mask for etching polysilicon in potassium hydroxide (KOH) solution heated at 20–25 °C. The SiNWs were formed by underetching the polysilicon with the Si_3N_4 mask for 15–20 min to achieve a width of around 150–300 nm for the 2 μm wide mask and 2–3 μm for the 5 μm mask. The mask was then removed by etching it in BHF solution for 8 min.

Step 4: An oxide was deposited and patterned on top of the SiNWs to enable liquid gate measurements and avoid current leakages from SiNW. For this purpose, a 5 nm thick layer of aluminum oxide (Al_2O_3) was deposited by the Atomic Layer Deposition (ALD) technique and was patterned by using photoresist as mask with the same pattern as for the PECVD Si_3N_4. The patterning was done by wet etching in BHF for 15 s.

Step 5: Wiring and metal contacts for the SiNWs were formed. To achieve this, 150 nm magnetron sputtered Titanium-Tungsten (TiW) and 150 nm e-beam evaporated Gold (Au) were deposited sequentially and patterned by a lift-off process. To improve the polysilicon contact with the metal an annealing step was done in nitrogen (N2) flow at 350° C for 1 h.

Step 6: Finally, the passivation of the electrodes was done by sputtering 200 nm of Si_3N_4 and patterning it by a lift-process. The passivation properties of the Si_3N_4 were improved by annealing the wafer at 450 °C for 30 min.

The schematic diagram of all the fabrication steps is shown in Fig. 1.

2.2. Secondary ions mass spectroscopy (SIMS)

To estimate the concentration of boron dopants in the deposited polysilicon secondary ion mass spectroscopy (SIMS) was done on a test wafer with a 50 nm thick polysilicon layer soon after deposition.

2.3. Underetching

After the underetching of polysilicon for the patterning of the SiNWs and the removal of the Si_3N_4 mask the width of the resulting SiNWs was measured in order to evaluate the uniformity of the wet etching process. The measurements were made by using a scanning electron microscope (SEM) Supra VP 40 supplied by Zeiss.

2.4. Contact annealing

To improve the contact of polysilicon with the metal electrodes and the stability of the resistance of the SiNWs an annealing step was carried out at 350 °C for 1 h. Two probe measurements were done on all the chips in order to measure the resistance through the SiNWs before and after the annealing step and quantify the improvement of the contact properties. The resistance was measured between the bonding pads connecting the nanowires to the outside world. Fig. 2 shows the image of one of the sensor devices, indicating the positions of the probes for one of the nanowires on the device.

2.5. Electrical characterization

To study the field effect behavior of the SiNW sensor, electrical characterization measurements in air were performed. The measurement setup consisted of two Keithley 2400 source meters that were connected to a PC through a National Instruments GBIP cable and were controlled by a LabVIEW program. In one characterization step the source-drain voltage (V_{DS}) was kept constant at 300 mV while the back gate voltage (V_{GS}) was swept from −8 V to +8 V. As a second characterization step the ohmic behavior of the SiNW was also tested

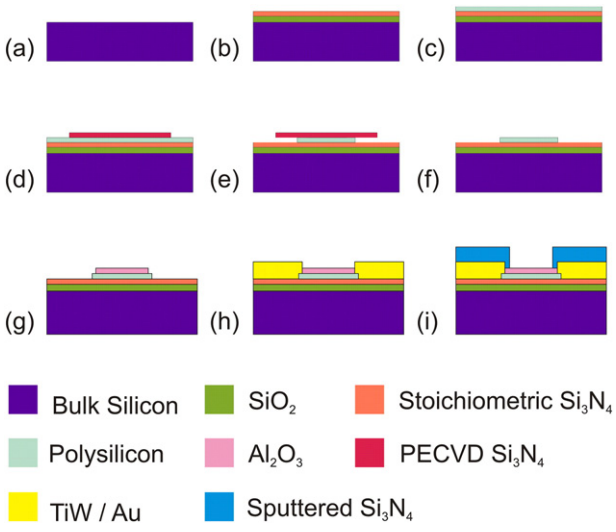

Fig. 1. Schematic images of the fabrication steps for the SiNW biosensor.

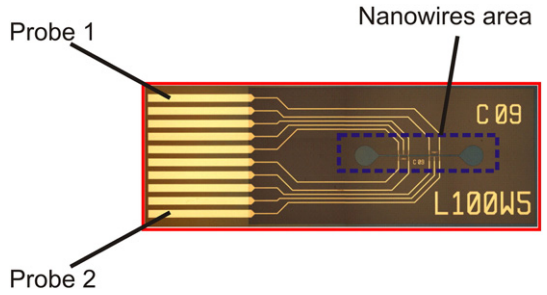

Fig. 2. Image of one of the sensor devices. The shown positions for the probes reflect measurement on one of the four nanowires on the chip. The position of the probes was changed accordingly to measure the resistance of the remaining nanowires.

by measuring the source-drain current (I_{DS}) vs (V_{DS}) at different back gate voltages. The schematic diagram of the electrical characterization setup is shown in Fig. 3.

The mobility constant and active dopant concentration were extracted using these electrical measurements.

2.6. Liquid gate characterization

To evaluate the performance of the SiNWs in liquids, which is necessary in order to use them as biosensors, liquid gate characterization was done by inserting the chip in a PMMA holder with a PDMS gasket which had an opening for insertion of liquid and a liquid gate electrode (a platinum wire). The platinum wire was fastened on top of the holder and 200 μl of phosphate buffer saline (PBS) solution was added on top of the chip until the holder was filled. The same measurement setup described in section 3.5 was also used for liquid gate characterization by switching the back gate with the liquid gate. Fig. 4 shows the schematic diagram of the setup.

2.7. pH sensing

The change of the SiNW resistance due to changes in the pH of the solution was monitored, in order to establish the sensing potential of the SiNWs. The Al_2O_3 on top of the nanowires was first functionalized using APTES. This was carried out by first washing the chips in absolute ethanol and drying them in a N_2 flow followed by oxygen plasma exposure for 2 min to activate the surface of the oxide with —OH terminated groups. The chips were then placed in a desiccator with N_2 flow, which was then placed on a hotplate at 60 °C. Two containers with 200 μl of APTES and 50 μl of DIPA were placed next to the chips in the desiccator. After 1 h of incubation the temperature of the hotplate was increased to

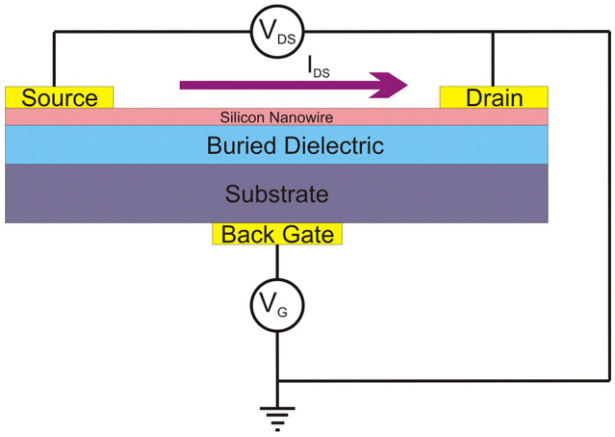

Fig. 3. Schematic diagram of the electrical setup used for electrical characterization of SiNW.

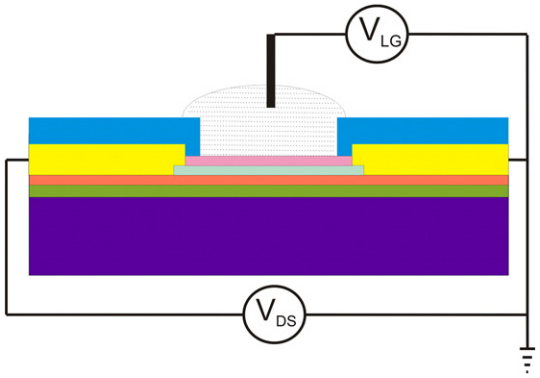

Fig. 4. Schematic diagram of the electrical setup used for liquid gate characterization of SiNW.

110 °C for 5 min. Fig. 5 shows the schematic diagram of the functionalization steps.

Five pH buffer solutions were prepared with values of 2.98, 4, 7.4, 9.21 and 10 as measured by a pH meter. After adding the buffer solutions to the functionalized chips the measurements were made by keeping the liquid gate at a potential of 0 V and the source-drain voltage (V_{DS}) at 300 mV while recording the source-drain current. The current was measured continuously over a period of 2 s (14 measurement points). The chip was washed with MilliQ water for 3 times with a pipette after a measurement with each buffer solution. In a second experiment, shorter (15 μm) and slightly narrower nanowires were tested with three pH solutions (4, 7 and 10). Here 1070 measurement points were obtained for 150 s before switching the pH solution. The gate voltage was set to 0 V.

3. Results & discussion

3.1. Secondary ions mass spectroscopy (SIMS)

One of the SIMS measurements made on the test wafer is shown in Fig. 6. The boron dopant concentration is found to be around 5×10^{18} atoms/cm^3. The increase in the dopant concentration at the bottom of the polysilicon layer is due to the fact that in the recipe of the furnace diborane (B_2H_6) gas, which is responsible for the induction of boron dopants in the polysilicon, is released first and the silane (SiH_4) gas which is decomposed in the furnace to deposit polysilicon on the substrate is released later. This results in the high dopant concentration of boron in the beginning which gets stabilized to the value of 5×10^{18} atoms/cm^3 as we move closer to the surface. This level of dopant concentration in polysilicon can provide better ohmic contact with metal [28,30]. The other spike which is close to the surface of the polysilicon is an artifact caused by the equipment, as it takes some time for it to give stable measurements.

To further confirm the suitability of this doping concentration we measured the current through the nanowire using an alternating

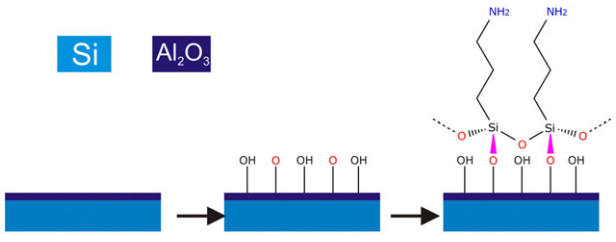

Fig. 5. Schematic diagram of the functionalization steps with APTES. After cleaning with ethanol and activating in oxygen plasma for 2 min, the oxide surface is now terminated with OH groups that are able to bind to the silane (APTES) in a subsequent step done at an elevated temperature in a nitrogen atmosphere.

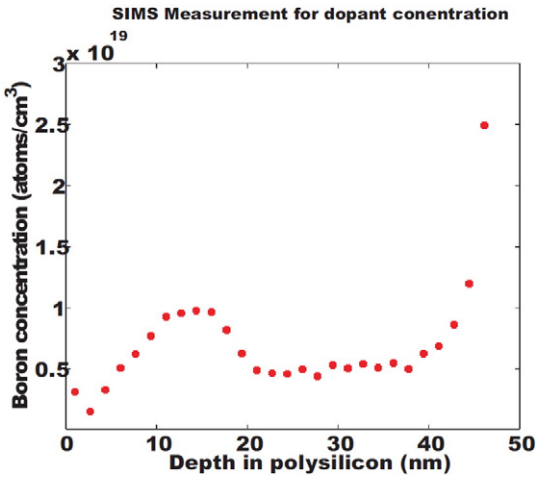

Fig. 6. Dopant distribution within the in-situ doped polysilicon as measured by SIMS (on x-axis 0 is the top surface of the polysilicon and 50 is the bottom).

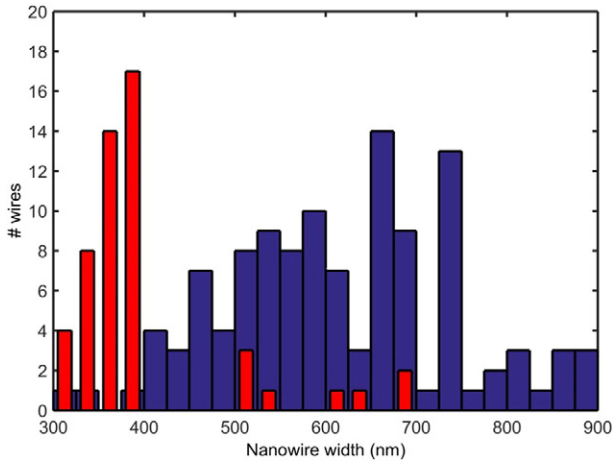

Fig. 8. Histogram of the width measurements of SiNW with 2 μm Si_3N_4 mask for two different wafer batches.

voltage source, and noted the phase shift between voltage and current. This was done for three different gas flows during deposition of the boron doped polysilicon. We confirmed that the flow used to provide the measured doping concentration resulted in no phase change, which indicates an ohmic contact. Smaller gas flows resulted in large phase change or no current flow at all.

3.2. Underetching

Fig. 7 shows SEM images of one of the SiNWs after removing the Si_3N_4 mask. Images like this were used for the width measurements. They also show that the nanowires do not have a homogeneous width along their length.

The width of all SiNWs on one wafer was measured to establish the reproducibility and uniformity of the KOH etch process forming the nanowires. The histogram of Fig. 8 shows the width distribution for the nanowires formed using the 2 μm wide mask for two different batches fabricated with a year in between by two different users.

It is clear from Fig. 8 that there are great differences in the obtained widths of the nanowires, not only between different wafer batches, but also within the wafer itself. The latter is rather unexpected, as wet etch processes tend to be rather homogeneous. However, it was observed that the SiNWs in the center of the wafer were etched slower compared to the ones in the edges. This can relate the observed non-uniformity of the SiNW widths to the dimensions of the Si_3N_4 mask used to create them. As the Si_3N_4 mask is made by dry etching, which is known to be non-uniform by as much as 20%, it is very likely that it is the differences in the dimensions of the mask that are largely responsible for the observed spreading in the SiNW widths. Regarding the batch to batch differences, the inhomogeneity there can be explained by considering the form of the KOH bath, which is warmed by a heating element at the edges of the bath and stirred with flow from the bottom of the tank. This can lead in concentration and temperature gradients that can explain some of the non-uniformity. Moreover, the bath is changed once every three months, and the etch rate is dependent on bath age and usage.

As the above parameters are not easily controlled, the wires are etched for a standard 12 min and checked in an optical microscope. After this step subsequent etches are done for 2 min at a time until the required width is reached. This can of course further lead to reproducibility issues, as it is up to the user to decide whether or not to stop the etching or continue it. Other underetching options that are less user-dependent exist, for example using dry etching techniques.

3.3. Contact annealing

The results of the two probe resistance measurements made before and after annealing on all the SiNWs are shown in Fig. 9.

From the measurements it is clear that the contact between polysilicon and gold electrodes has been greatly improved after annealing. It was also observed during the measurements that the resistance values were not stable before annealing due to loose contact between polysilicon and gold, but this improved after the annealing of the contacts. A possible explanation is that at higher temperatures the TiW forms ternary silicide by reacting with Si which improves the contact resistance and stabilizes the electrical connection [31]. At the same time

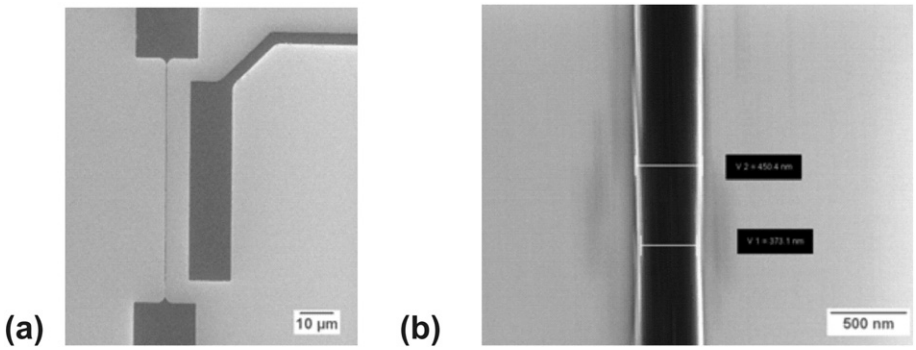

Fig. 7. SEM image of the 370 nm wide SiNW (a) With source-drain and side gate (b) zoomed in image.

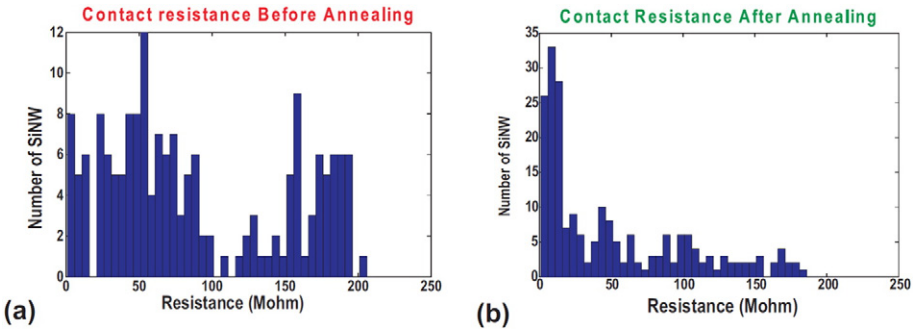

Fig. 9. The resistance of the SiNWs before and after annealing. It is clear that the contact after annealing is significantly improved.

TiW also acts as a barrier between Au and Si. When TiW is not present precipitation of Si [32,33] occurs which causes disconnection between source and drain.

3.4. Electrical characterization

Fig. 10 shows the source-drain current (I_{DS}) measured against backgate voltage sweep when the source-drain voltage (V_{DS}) was kept

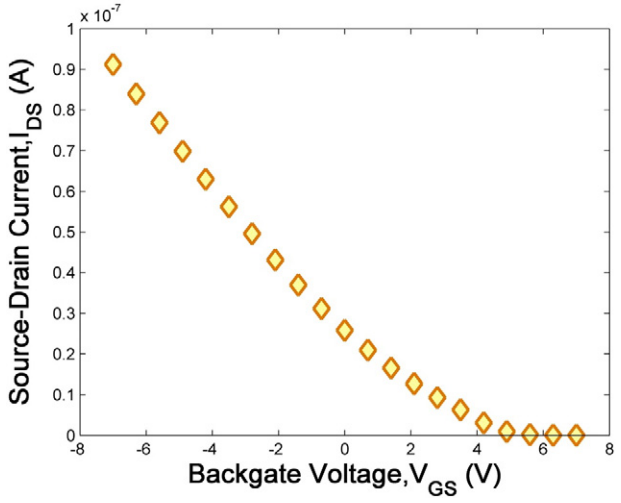

Fig. 10. The change in source-drain current (I_{DS}) in a SiNW with dimension length × width × thickness = 70 μm × 0.4 μm × 0.2 μm when sweeping the back gate voltage from −8 V to +8 V while keeping the source-drain voltage (V_{DS}) at 300 mV.

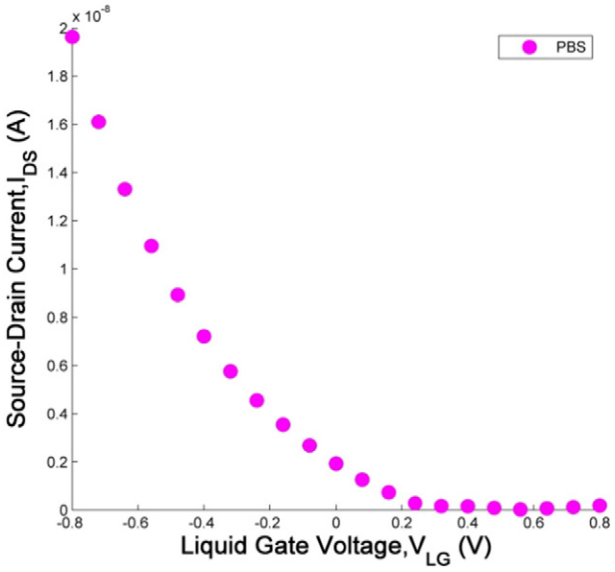

Fig. 12. Source-drain current (I_{DS}) response of SiNW by sweeping liquid gate voltage (V_{LG}) in PBS solution.

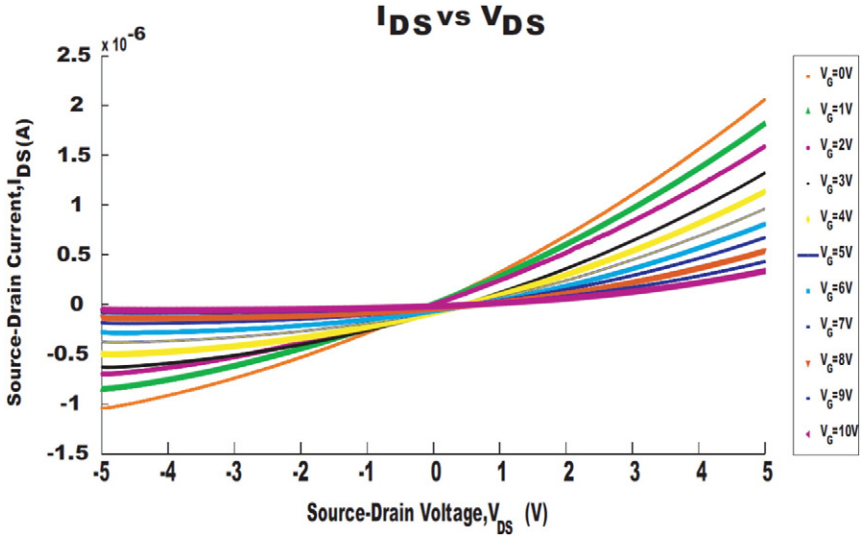

Fig. 11. The source-drain current (I_{DS}) as a function of source-drain voltage (V_{DS}) at different back gate potentials (V_{BG}).

at a constant value of 300 mV. This measurement was done in air with the purpose of showing that the devices have a transistor behavior, don't exhibit leakage and are able to be fully depleted.

The full depletion in the SiNW is achieved at around 5 V, whereas the subthreshold regime is reached at around 3 V. Using the slope of the linear part of the curve in Fig. 10 the mobility constant was calculated by using the formula

$$\mu_p = \frac{L \times \alpha}{C' V_{DS} W}$$

where μ_p is the mobility constant, L is the length of SiNW, W is the width of SiNW, α is the slope of the curve, and V_{DS} is the source-drain voltage. The mobility value was found to be 3.594 cm^2/Vs and using this value in the equation below the active dopant concentration was found to be 7.55×10^{17} atoms/cm^3.

$$p_{0=} \frac{KL}{W\mu_p q t V_{DS}}$$

where p_0 is the dopant concentration, $K$is the source drain current at 0 V back gate voltage, V_{DS} is the source drain voltage, t is the thickness, q is the electric charge, L is the length and W is the width of the SiNW.

The calculated values for the doping concentration are a bit smaller than what was found by the SIMS measurements. However, one should consider that the nanowires used for the characterization are made after a 1 min oxidation at 1100 °C to reduce their height, which will inevitably also have an effect on the concentration of dopants. It is therefore expected that the calculated doping concentration is smaller than the one measured by SIMS.

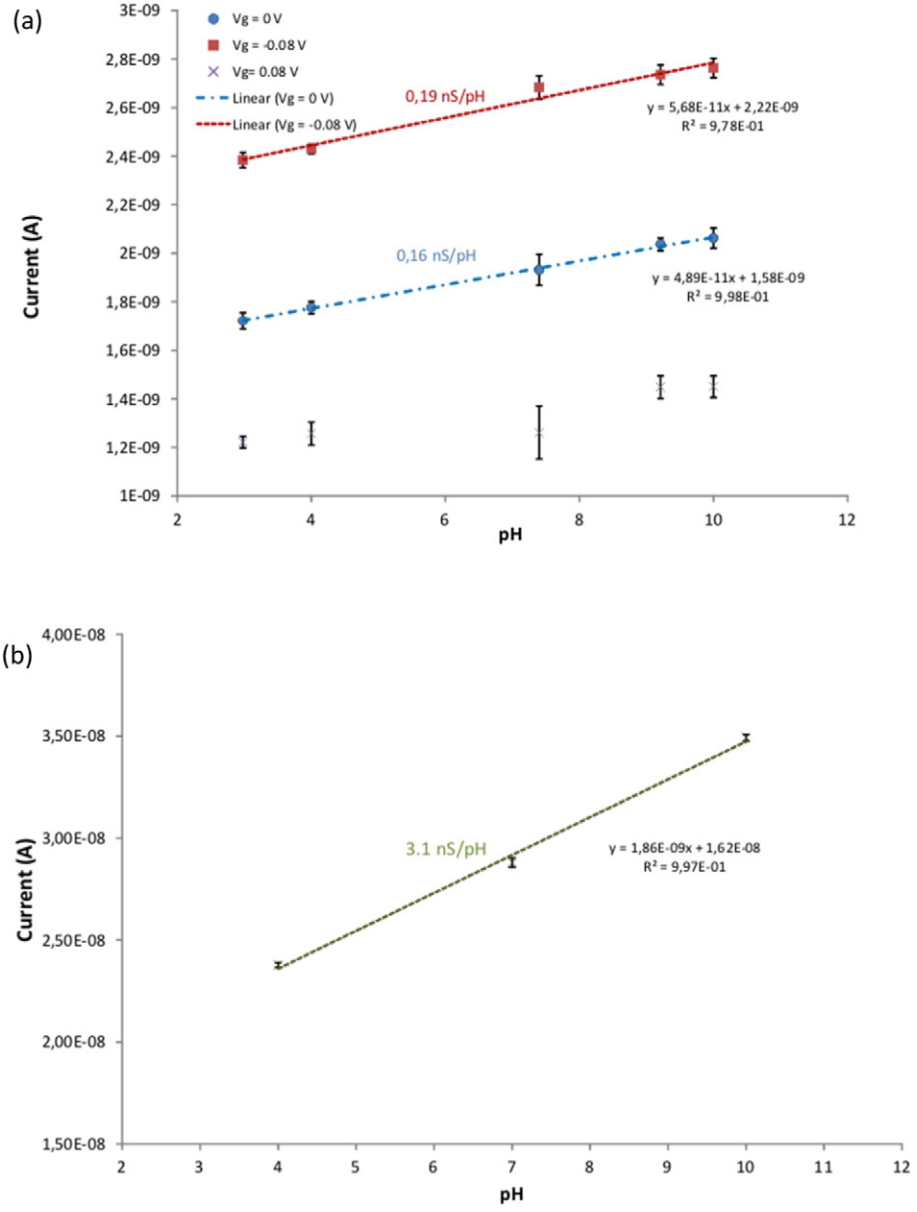

Fig. 13. (a) Change in source-drain current (I_{DS}) at different pH buffer solutions for a 400 nm wide nanowire at three different gate voltages. As the gate voltage approaches the full depletion value, the current is around the noise level and the measurements are not reliable. (b) Change in source-drain current at different pH buffer solutions for a 300 nm wide nanowire with an 8 times shorter length than in (a). The current is one order of magnitude higher.

Furthermore the calculated mobility value is found to be quite close to the ones already reported for polycrystalline silicon with the above mentioned level of dopant concentration [34,35].

The voltage controlled resistance measurements are shown in Fig. 11. From the results it is observed that the external gate has a bigger influence on the resistance of the SiNW. The saturation is achieved in the negative source-drain voltage which is due to the fact that the surface potential at the source end is smaller than that at the drain end, whereas the gate potential is the same all over the SiNW. This potential difference between gate and source is greater than the difference between gate and drain and makes the electric field larger at the source end compared to the drain [36].

3.5. Liquid gate characterization

The purpose of the liquid gate characterization was to verify that the dielectric properties of Al_2O_3 are stable enough to avoid any current leakage from the SiNW into the liquid and to check if the SiNW can still be depleted by applying a liquid gate. Fig. 12 shows that the SiNW can be fully depleted at a liquid gate voltage of around 0.25 V. No current leakage was observed during the liquid gate sweep, which proves the stability of Al_2O_3 as a dielectric for this sensor. We note that if the SiNW is protected only by the native oxide growing on it, then there is leakage through the native oxide to the liquid even at very small liquid gate voltages.

The fact that the nanowire can be depleted at such a low voltage means that its use in a POC device is possible, as these are usually battery operated. We note, however, that the current through the nanowire is only a few nA, which means that good amplifiers are needed to get a good readout signal, although this current value can be increased by as much as a factor of 15 by reducing the nanowire length.

3.6. pH sensing

To prove that the in situ doped polysilicon SiNWs can be used as biosensors, a pH sensing experiment was conducted with APTES functionalized SiNW. Fig. 13(a) shows the current through a single SiNW at five pH buffer solutions. The response of the SiNW is in accordance to the expectations because at pH values less than 7, positive charges are the dominant charges in the solution and they influence the p-type SiNW by repelling the charge carriers in the SiNW, i.e. the SiNW resistance increases. The lower the pH value the higher the resistance and the smaller the current. Above pH 7 the negative charges are dominant and therefore the resistance decreases with a current increase as a result.

The response of the SiNWs is linear in the range of tested pH values which is also in accordance to the already reported works [1,16,37–39]. The SiNW in Fig. 13(a) shows a change of 0.049 nA/pH, which corresponds to 0.16 nS/pH. Previous works have shown a larger response, but on considerably shorter and narrower nanowires. The fact that the nanowires in this work are relatively wide and long is certainly not an advantage in terms of biosensing, but the results show that even such wires are able to perform satisfactorily. We note that when slightly changing the gate voltage the sensitivity increases slightly to 0.19 nS/pH. This is most likely due to the nanowire being closer to the subthreshold regime for this gate voltage, as established in [37]. In a recent preliminary experiment, eight times shorter but only slightly narrower nanowires were used to determine the sensitivity in pH (Fig. 13(b)). The results show indeed an eight times larger current passing through the nanowires and a much increased sensitivity to pH, which at 3.1 nS/pH is extremely close to the 5 nS/pH reported in e.g. [39] for an e-beam fabricated single crystalline silicon nanowire. However, more experiments are underway to confirm this result.

The experiment of Fig. 13(a) was repeated with a different nanowire from the same batch, immediately after APTES functionalization (measurement 1) and a week after (measurement 2), with the nanowire left in air at room temperature between measurements. As can be seen in Fig. 14, the pH response was linear immediately after functionalization (with a response of 0.12 nA/pH or 0.4 nS/pH), exactly like in Fig. 13, but became exponential after a week.

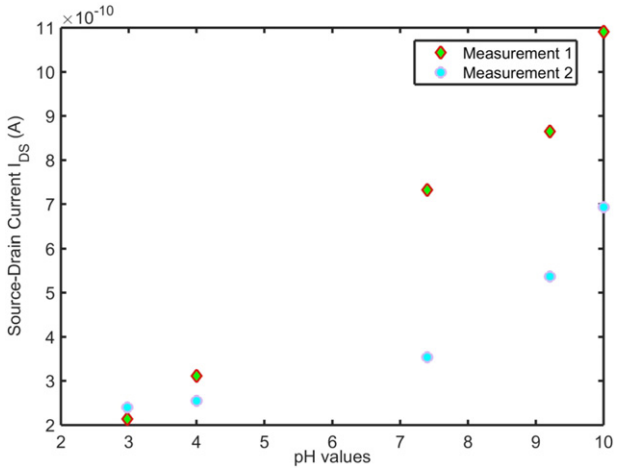

Fig. 14. Change in source-drain current (I_{DS}) at different pH buffer solutions immediately after functionalization with APTES (measurement 1) and a week after functionalization (measurement 2).

The nanowire response a week after functionalization resembles the response observed from a non-functionalized nanowire (as seen in [1]). Considering that APTES is not particularly stable in air, it is logical to assume that the functionalization was simply removed during measurement 2 and the response measured was that of a non-functionalized wire, as reported in [1]. This creates a few issues regarding the stability of the sensor under ambient conditions, and more investigations need to be done in order to ensure that the functionalization layer is not removed when the sensor is stored. However, APTES is known to be stable when the nanowire chips are stored either in a nitrogen atmosphere or simply immersed in ethanol. We are in the process of evaluating these methods.

4. Conclusion

A novel fabrication technique for low-cost and robust fabrication of SiNWs biosensors by using in-situ boron doped polysilicon in a junctionless setup has been developed which involves standard UV photolithography and wet KOH etch to pattern SiNWs. The characterization of the fabrication process has shown that the process has a high yield and reproducibility. The electrical characterization and liquid measurements have shown that the electrical properties of the SiNWs sensors are comparable to the already demonstrated sensors. The successful detection of different pH buffer solutions with APTES functionalized SiNWs shows that the sensor has a potential to be used in a POC setup for the detection of biomolecules, if the issues with the stability of the functionalization layer are resolved.

Acknowledgements

The authors would like to thank Professor Ole Hansen for his expert advices on fixing the problems during the fabrication process and Danchip cleanroom staff for providing all the support on different equipments. This project is a part of the EU Marie Curie Initial Training Networks (ITN) Biomedical engineering for cancer and brain disease diagnosis and therapy development: EngCaBra. Project no. PITN-GA-2010-264417.

References

[1] Y. Cui, et al., Nanowire nanosensors for highly sensitive and selective detection of biological and chemical species, Science 293 (5533) (2001) 1289–1292.

[2] F. Patolsky, et al., Electrical detection of single viruses, Proc. Natl. Acad. Sci. U. S. A. 101 (39) (2004) 14017–14022.
[3] J. Hahm, C.M. Lieber, Direct ultrasensitive electrical detection of DNA and DNA sequence variations using nanowire nanosensors, Nano Lett. 4 (1) (2004) 51–54.
[4] G.F. Zheng, et al., Multiplexed electrical detection of cancer markers with nanowire sensor arrays, Nat. Biotechnol. 23 (10) (2005) 1294–1301.
[5] D. Kwasny, et al., Nanoscaled Biological Gated Field Effect Transistors for Cytogenetic Analysis. 2014 9th Ieee International Conference on Nano/Micro Engineered and Molecular Systems (Nems), 2014 130–134.
[6] B. Srinivasan, S. Tung, Development and applications of portable biosensors, Jala 20 (4) (2015) 365–389.
[7] M. Holzinger, A. Le Goff, S. Cosnier, Nanomaterials for biosensing applications: a review, Frontiers in Chemistry 2 (2014).
[8] K.K. Jain, Applications of nanobiotechnology in clinical diagnostics, Clin. Chem. 53 (11) (2007) 2002–2009.
[9] R. Seigneuric, et al., From nanotechnology to nanomedicine: applications to cancer research, Current Molecular Medicine 10 (7) (2010) 640–652.
[10] C.P.Y. Chan, et al., Evidence-based point-of-care diagnostics: current status and emerging technologies, in: R.G. Cooks, J.E. Pemberton (Eds.), Annual Review of Analytical Chemistry, Vol 6, Annual Reviews, Palo Alto 2013, pp. 191–211.
[11] L.M. Bellan, D. Wu, R.S. Langer, Current trends in nanobiosensor technology, Wiley Interdisciplinary Reviews-Nanomedicine and Nanobiotechnology 3 (3) (2011) 229–246.
[12] D.V. Lim, et al., Current and developing technologies for monitoring agents of bioterrorism and biowarfare, Clin. Microbiol. Rev. 18 (4) (2005) 583-+.
[13] F. Patolsky, G.F. Zheng, C.M. Lieber, Fabrication of silicon nanowire devices for ultrasensitive, label-free, real-time detection of biological and chemical species, Nat. Protoc. 1 (4) (2006) 1711–1724.
[14] E. Stern, et al., Label-free immunodetection with CMOS-compatible semiconducting nanowires, Nature 445 (7127) (2007) 519–522.
[15] X.T. Vu, et al., Fabrication and application of silicon nanowire transistor arrays for biomolecular detection, Sensors and Actuators B-Chemical 144 (2) (2010) 354–360.
[16] O. Knopfmacher, et al., Nernst limit in dual-gated Si-nanowire FET sensors, Nano Lett. 10 (6) (2010) 2268–2274.
[17] N. Elfstrom, A.E. Karlstrom, J. Linnros, Silicon nanoribbons for electrical detection of biomolecules, Nano Lett. 8 (3) (2008) 945–949.
[18] A. Vacic, et al., Multiplexed SOI BioFETs, Biosens. Bioelectron. 28 (1) (2011) 239–242.
[19] I. Park, et al., Top-down fabricated silicon nanowire sensors for real-time chemical detection, Nanotechnology (2010) **21**(1).
[20] N. Lu, et al., CMOS-compatible silicon nanowire field-effect transistors for ultrasensitive and label-free microRNAs sensing, Small 10 (10) (2014) 2022–2028.
[21] G.J. Zhang, et al., An integrated chip for rapid, sensitive, and multiplexed detection of cardiac biomarkers from fingerprick blood, Biosens. Bioelectron. 28 (1) (2011) 459–463.
[22] H.D. Tong, et al., Novel top-down wafer-scale fabrication of single crystal silicon nanowires, Nano Lett. 9 (3) (2009) 1015–1022.
[23] G. Jayakumar, et al., Silicon nanowires integrated with CMOS circuits for biosensing application, Solid State Electron. 98 (2014) 26–31.
[24] M.M.A. Hakim, et al., Thin film polycrystalline silicon nanowire biosensors, Nano Lett. 12 (4) (2012) 1868–1872.
[25] G.J. Zhang, et al., Highly sensitive measurements of PNA-DNA hybridization using oxide-etched silicon nanowire biosensors, Biosens. Bioelectron. 23 (11) (2008) 1701–1707.
[26] G.J. Zhang, et al., DNA sensing by silicon nanowire: charge layer distance dependence, Nano Lett. 8 (4) (2008) 1066–1070.
[27] M.C. Chen, et al., A CMOS-compatible poly-Si nanowire device with hybrid sensor/memory characteristics for system-on-chip applications, Sensors 12 (4) (2012) 3952–3963.
[28] J.P. Colinge, et al., Nanowire transistors without junctions, Nat. Nanotechnol. 5 (3) (2010) 225–229.
[29] R. Rogel, et al., Polycrystalline silicon nanowires synthesis compatible with CMOS technology for integrated gas sensing applications, IEEE Transactions on Electron Devices 61 (2) (2014) 598–604.
[30] J.P. Gambino, E.G. Colgan, Silicides and ohmic contacts, Mater. Chem. Phys. 52 (2) (1998) 99–146.
[31] S.E. Babcock, K.N. Tu, Titanium-tungsten contacts to SI - the effects of alloying on SCHOTTKY contact and on silicide formation, J. Appl. Phys. 53 (10) (1982) 6898–6905.
[32] S.Q. Wang, et al., Diffusion barrier properties of TiW between Si and Cu, J. Appl. Phys. 73 (5) (1993) 2301–2320.
[33] P. Wiklund, et al., TiW and Al contacts to shallow P+ junctions - a comparison between furnace and rapid thermal annealing (RTA), J. Phys. 49 (C-4) (1988) 489–493.
[34] D.P. Joshi, R.S. Srivastava, Mobility and carrier concentration in polycrystalline silicon, Solar Cells 12 (3) (1984) 337–344.
[35] J.Y.W. Seto, The electrical properties of polycrystalline silicon films, J. Appl. Phys. 46 (12) (1975) 5247–5254.
[36] The Electronics Handbook, Second edition ed, . Electrical Engineering Handbook, Taylor and Francis, 2005.
[37] X.P.A. Gao, G.F. Zheng, C.M. Lieber, Subthreshold regime has the optimal sensitivity for nanowire FET biosensors, Nano Lett. 10 (2) (2010) 547–552.
[38] N. Elfström, Silicon Nanowires for Biomolecule Detection, KTH, Stockholm, 2008.
[39] Y. Chen, et al., Silicon-based nanoelectronic field-effect pH sensor with local gate control, Appl. Phys. Lett. 89 (22) (2006).